

# CARACTERIZAREA FILMELOR VITROASE DOPATE CU CdS, OBȚINUTE PRIN DEPUNERE CU LASER PULSAT

## CHARACTERIZATION OF CdS-DOPED GLASS FILMS OBTAINED BY PULSED LASER DEPOSITION

C. R. IORDĂNESCU<sup>1</sup> (ȘTEFAN), M. ELIȘA<sup>1\*</sup>, G. EPURESCU<sup>2</sup>, M. FILIPESCU<sup>2</sup>, M. ENCULESCU<sup>3</sup>,  
R.C.C. MONTEIRO<sup>4</sup>, L. CONSTANTIN<sup>1</sup>

<sup>1</sup> National Institute of R&D for Optoelectronics INOE 2000, Magurele, PO Box MG-5, 77125, Romania

<sup>2</sup> National Institute for Laser, Plasma and Radiation Physics, Magurele, Romania

<sup>3</sup> National Institute of Materials Physics, Magurele, Romania

<sup>4</sup> Faculty of Sciences and Technology, Universidade Nova de Lisboa, Caparica, Portugal

*In the present work we study the optical, structural and morphological properties of CdS-doped glass films, deposited by Pulsed Laser Deposition (PLD) method. The glass target used for ablation was prepared by conventional melt-quenching technique and the semiconductor dopant, CdS powder, was embedded in the borosilicate melt glass host by continuous stirring. In order to improve the properties of the films, the laser wavelength was modified. Photoluminescence emission (PL) of CdS-doped glass films revealed a broad band located in the visible range. The structural analysis was carried out by micro-Raman spectroscopy, pointing out specific vibration modes for Si-O-Si bonds as well as for CdS dopant. The morphology and the chemical characterization of the films were investigated by Scanning Electron Microscopy (SEM), Energy Dispersive X-ray spectroscopy (EDX) and Atomic Force Microscopy (AFM).*

*În prezenta lucrare au fost studiate proprietățile optice, structurale și morfologice ale filmelor vitroase dopate cu CdS, obținute prin tehnica de depunere cu laser pulsat. Ținta de sticlă utilizată pentru ablație a fost obținută prin metoda convențională de topire-răcire iar dopantul semiconductor, pulberea de CdS, a fost introdusă în topitura vitroasă borosilicatică prin omogenizare continuă. În scopul îmbunătățirii proprietăților filmelor, a fost modificată lungimea de undă a laserului folosit la ablație. Emisia fotoluminescentă a filmelor vitroase dopate cu CdS a prezentat o bandă largă localizată în domeniul vizibil. Analiza structurală a fost efectuată prin spectroscopie Raman, evidențiindu-se moduri de vibrație specifice legăturilor Si-O-Si precum și cele ale dopantului, CdS. Morfologia și caracterizarea chimică a filmelor au fost investigate prin Microscopie Electronică de Baleiaj (SEM), Spectroscopie de Energie Dispersă de Raze X (EDS) și Microscopie Atomică de Forță (AFM).*

**Keywords:** borosilicate glass, thin film, pulsed laser deposition, luminescence, CdS-doped glass

### 1. Introduction

Cadmium sulfide (CdS) is an important II-VI semiconductor with many excellent physical and chemical properties, being a promising material for applications in optoelectronic devices, such as lasers, detectors for lasers, solar cells, photo-sensors, optical wave-guides and non-linear integrated optical devices [1-8]. An extension of the application range of II-VI semiconductor nanoparticles is reported in previous articles [9-12], where optical transparent matrices are used as vitreous host or organic polymer host.

The pulsed laser deposition (PLD) has become an appealing growth technique of thin films of wide band gap materials with high PL efficiency [13]. There are several gains of PLD method related to the deposition of high quality thin films, such as: relatively low substrate temperature, the preserved stoichiometry of the deposited layers and

the possibility of controlling the growth rate through adjusting the pulses repetition rate and fluency of the laser beam [14]. Nanotwinning and structural phase transition in CdS quantum dots deposited on different substrates as a result of different annealing temperatures were recently reported [15,16].

In particular, evidence of near band gap emission at room temperature from CdS films deposited by PLD has been reported [13].

A study on the effect of substrate temperature on the formation of CdO composite in CdS-doped SiO<sub>2</sub> films deposited by PLD was reported [17].

In the present paper, optical, structural and morphological properties of CdS-doped glass films were investigated in dependency on PLD deposition parameters. These doped films have application in temperature sensing based on luminescence characteristics.

\* Autor corespondent/Corresponding author,  
E-mail: [astatin18@yahoo.com](mailto:astatin18@yahoo.com)

## 2. Experimental

The CdS-doped glass was prepared by a wet non-conventional melting-quenching method, using powder analytical grade reagents and providing a continuous mechanical stirring of the melt in order to improve the chemical and optical homogeneity of the final material. The CdS-doped silicate glass was mechanically processed to obtain a target of 50.8 mm diameter and 5 mm thickness, the deposition being made on P-type Si (100) substrate of 1 cm<sup>2</sup> area. In the case of the film from experiment 1, the deposition was also made on quartz substrate in order to measure the optical absorption in transmission mode.

In order to improve the properties of the films, some PLD parameters were modified: pulse number and laser wavelength (see Table 1). The chemical composition of CdS-doped glass (wt. %) was investigated by X-Ray Fluorescence (XRF) analysis, with PANalytical XRF-WDS 4 kW AXIOS sequential spectrometer (Rh X-ray tube) under He flow. Optical absorption was recorded by UV-Vis-NIR spectrophotometry (PerkinElmer Lambda 1050). The structural analysis was carried out by Raman spectroscopy (micro-Raman LabRAM HR 800, Horiba Jobin-Yvon). Photoluminescence behavior of the deposited film was investigated by Nanolog 3 spectrofluorometer, Horiba Jobin-Yvon. The morphology and elemental composition of the films were evaluated using an EVO 50XVP Carl Zeiss Scanning Electron Microscope (SEM), equipped with Energy-Dispersive X-ray (EDX) Quantax Bruker 200 analyzer, as well as by Atomic Force Microscopy (AFM), XE100 Park System. The thickness of the deposited films was measured using a surface profilometer (Dektak 150).

The films were deposited using 15 rpm substrate rotation speed, 20 rpm target rotation speed and target to substrate distance 6 cm.

## 3. Results and discussion

### 3.1. XRF analysis

The oxide composition (wt. %) of CdS-doped glass target provided by XRF analysis is presented in the Table 2. The vitreous network formers are SiO<sub>2</sub> and B<sub>2</sub>O<sub>3</sub> and the vitreous network modifiers are Na<sub>2</sub>O, K<sub>2</sub>O and CaO. The amount of CdS dopant from the starting glass target was analyzed in connection with amount of CdO and SO<sub>3</sub> compounds.

### 3.2. UV-VIS absorbance

Figure 1 shows the absorbance spectrum (UV-Vis-NIR) of CdS-doped film deposited on quartz substrate (experiment 1) compared with the absorption spectrum of quartz substrate and that of the undoped borosilicate glass target. It was found that the absorption edge of the deposited film is shifted toward higher wavelength due to the semiconductor dopant particles embedded in the

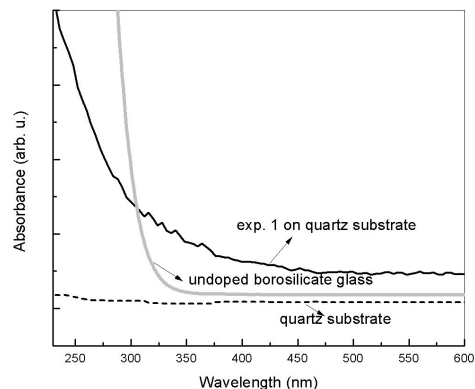
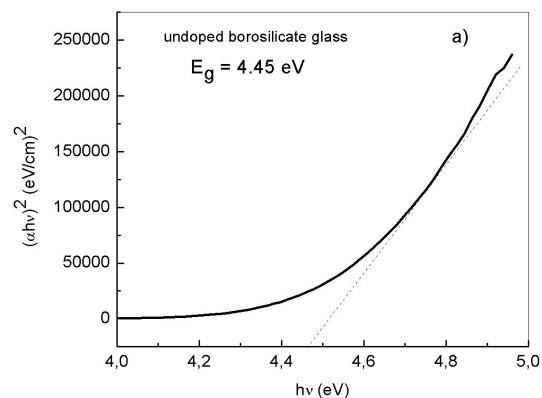
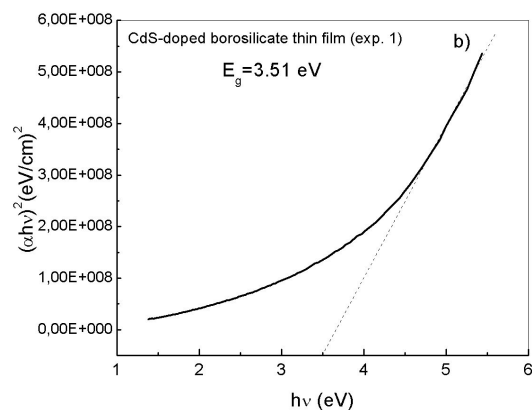


Fig. 1 - The UV-Vis absorption spectrum of CdS-doped film on quartz substrate (experiment 1) compared with the absorption spectrum of undoped glass and quartz substrate / *Spectrul de absorbție UV-Vis al filmului dopat cu CdS depus pe substrat de cuarț (experimentul 1) comparativ cu spectrul de absorbție al sticlei nedopate și cel al substratului de cuarț.*



A



B

Fig. 2 -  $(\alpha hv)^2$  versus  $h\nu$  of a) undoped borosilicate glass and b) CdS-doped glass deposited on quartz, in experiment 1.  $(\alpha hv)^2$  în funcție de  $h\nu$  pentru: a) sticla borosilicatică nedopată și b) sticla dopată cu CdS depusă pe cuarț, în experimentul 1.

glass matrix, according to the literature data [18].

The absorbance of the quartz substrate is very low, almost constant with wavelength change, suggesting that the substrate has an insignificant influence on the optical absorbance of the film.

The thickness of the deposited film from experiment 1 is 1.75  $\mu\text{m}$  and that from experiment 2 is 1.27  $\mu\text{m}$ , measured by profilometry method.

The CdS-doped film bandgap was calculated by plotting  $(ahv)^2$  vs.  $hv$  ( $hv$  is the photon energy) as described in literature [19] and presented in Figure 2. The linear part of the plot was extrapolated for  $(ahv)^2 = 0$ , resulting a band gap value,  $E_g^{(eff)} = 3.51$  eV, corresponding to 353 nm. Similarly, the band gap of the undoped borosilicate glass was calculated, being 4.45 eV corresponding to a lower wavelength, 278 nm. So, the absorption edge is shifted toward higher wavelength, lower energy, in the case of CdS-doped film.

The energy band gap dependency on the size of semiconductor nanoparticles is approximated using the equation (1) [20]:

$$E_g^{(eff)} = E_g^{(bulk)} + \frac{h^2}{2m^*d^2} \quad (1)$$

where,  $E_g^{(eff)}$  is the energy band gap of the nanoparticles,  $E_g^{(bulk)}$  is the energy band gap of a bulk semiconductor,  $h$  is the Planck constant,  $m^*$  is the reduced mass of exciton, calculated based on the effective mass of electrons and holes (0.19 $m_0$  and 0.8 $m_0$  respectively, where  $m_0$  is the free electron mass) [21],  $d$  is the nanocrystal size, the energy band gap of the bulk semiconductor  $E_g^{(bulk)} = 2.42$  eV. It was found that the diameter of the nanoparticles is about 3.8 nm.

### 3.3. Fluorescence analysis

In Figure 3 the photoluminescence (PL) spectrum of CdS-doped glass target is presented as compared with the PL spectrum of CdS-doped film on silicon substrate (experiment 2), both of them provided by 450 nm excitation, using a 450 nm optical band-pass filter on emission path.

PL spectra of the glass target and the deposited film from experiment 2 showed broad bands in the visible range (peaks around 630 nm and, respectively, 655 nm) specific to the electrons in the conduction band, excitonic states and trap states. Luminescence is very sensitive to the nature of nanoparticle surface due of the presence of gap surface states arising from surface non-stoichiometry and unsaturated bonds [19]. In CdS, defects consists of cadmium vacancies, sulphur vacancies, interstitial cadmium and sulphur atoms adsorbed on the surface [22]. The FWHM (Full Width at Half Maximum) of the glass target is approximately 160 nm, due to the large range of semiconductor particles size. The glass target was previously heat treated at 600 °C for 2h in order to promote the growth of the dopant particles,

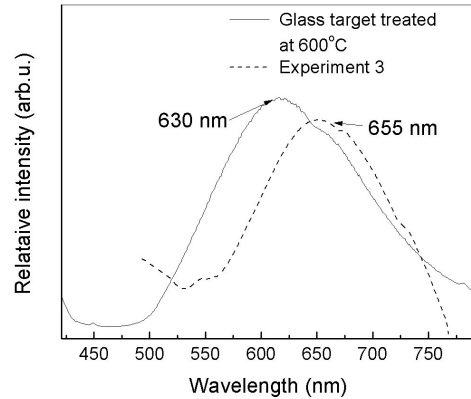


Fig. 3 - PL spectra of glass target and CdS-doped film (experiment 2) provided by 450 nm excitation. Spectrele de fotoluminescență (PL): al țintei de sticlă și al filmului dopat cu CdS (experiment 2), obținute prin excitare la 450 nm.

enhancing the visible emission. It was found that the films deposited in the experiment 1, operating at 248 nm laser wavelength revealed low intensity PL bands, not presented in this paper, that are in agreement with previous articles [23, 24]. In the case of the film obtained in experiment 2, it was noticed a PL band with the FWHM of about 119 nm, fitted by Gauss function. Based on FWHM values, PL band of the film from experiment 2 certifies the presence of CdS dopant particles, having a reduced size range by comparison with the glass target, as a consequence of the ablation deposition process. The intensity of the emission band in the case of the deposited film is lower than in the case of the bulk doped glass, taking into account the reduced amount of phosphors, meaning CdS particles embedded in the thin vitreous layer. With decreasing size of the nanocrystallites, the density of the surface states would increase as a result of increase in surface to volume ratio. Consequently, the luminescence is found to be dominated by surface state transitions rather than excitonic transitions [19].

### 3.4. Raman analysis

Figure 4 presents Raman spectra of the silicate glass target, silicon substrate and borosilicate films doped with CdS (experiments 1 and 2), by 514 nm Ar laser excitation. It can be seen that the spectrum of the CdS-doped film from experiment 1 reveals a similar pattern with the glass target, meaning that the deposition process preserved the structural features of the starting vitreous material. There were found rocking, bending and stretching vibration modes for Si-O-Si bonds as follows: 350  $\text{cm}^{-1}$  attributed to non-bridging silicon-oxygen bonds, 560  $\text{cm}^{-1}$  assigned to bending vibration and rocking vibration modes, 680  $\text{cm}^{-1}$  ascribed to Si-O-Si bending and 1100  $\text{cm}^{-1}$ , related to the asymmetric stretching vibration

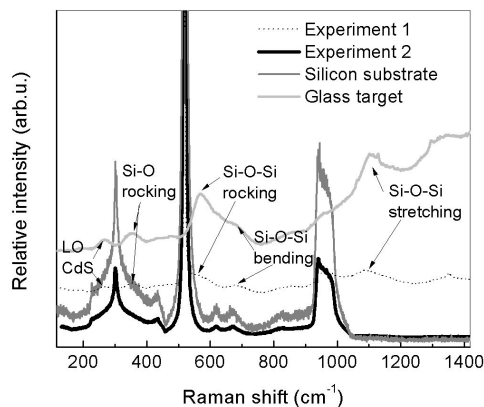


Fig. 4 - Raman spectra of: glass target, silicon substrate and CdS-doped films from experiments 1 and 2, provided by 514 nm laser excitation / Spectrele Raman: al țintei de sticlă, al substratului de siliciu și ale filmelor dopate cu CdS, din experimentele 1 și 2, obținute prin excitare laser la 514 nm.

mode [25, 26]. A Raman band at about 260 cm<sup>-1</sup> specific to longitudinal optical phonon (LO) of Cd-S bond, was found for the film from experiment 1, as reported in [27, 28]. This maximum was not found in the case of the experiment 2, probably, due to the lower thickness of the film allowing the silicon substrate to cover the signal of the CdS vibration mode. Others peaks noticed in the spectra are specific to silicon vibration modes [29, 30].

### 3.5. SEM image

In Figure 5, SEM images of CdS-doped films deposited on silicon substrate, experiments 1 and 2 are shown. SEM image of CdS-doped film from experiment 1 shows spherulitic units specific to PLD films, with size that is varying between 0.5-3 μm. A densification of the spherulitic units is found in the case of the film from experiment 1, possibly due to the increasing of the laser energy (decreasing the laser wavelength – see the Table 1) and, taking into consideration that 248 nm

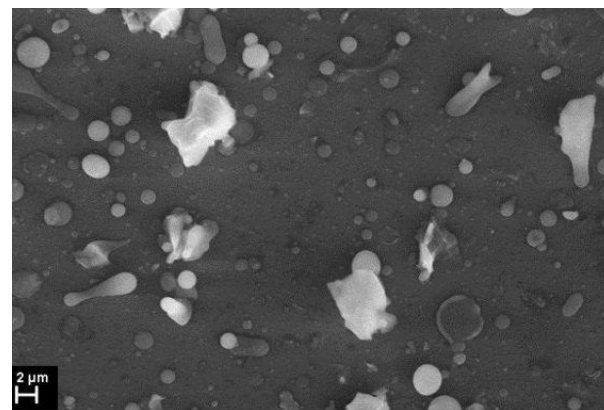
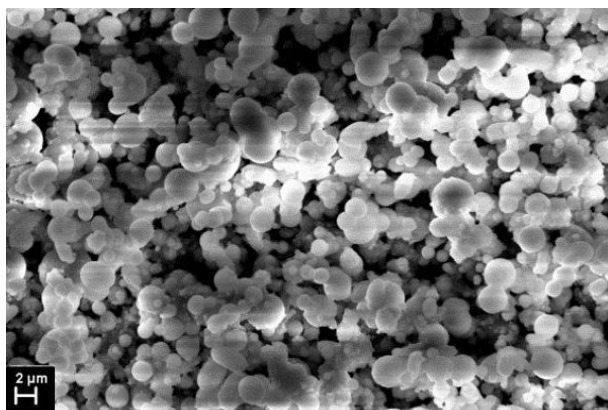


Fig. 5 - SEM images of CdS-doped films: (a) film experiment 1; (b) film experiment 2. Imaginile SEM ale filmelor dopate cu CdS: a) experimentul 1; b) experimentul 2.

Table 1

PLD experiments developed by varying different parameters (pulse number and laser wavelength) / Experimentele de depunere cu laser pulsant, desfășurate prin modificarea diferiților parametri (numărul de pulsuri și lungimea de undă laser)

Experiment no.	Substrate	Frequency (Hz) / Pulse number	Background pressure (Torr)	Substrate temperature (°C)	Laser wavelength (nm)
1	Silicon/Quartz	10 Hz/40000	4 × 10 <sup>-6</sup>	Room temperature	248
2	Silicon	10 Hz/128000	4 × 10 <sup>-6</sup>	Room temperature	1064

Table 2

The oxide composition (wt. %) of CdS-doped glass target provided by XRF analysis / Compoziția oxidică (% grav.) a țintei de sticlă dopată cu CdS, obținută din analiza de fluorescență cu raze X (XRF)

Oxide	Na <sub>2</sub> O	SiO <sub>2</sub>	K <sub>2</sub> O	CaO	CdO	SO <sub>3</sub>	B <sub>2</sub> O <sub>3</sub>
Composition (wt. %)	1	60	15	16	0.3	0.07	7

Table 3

EDX analysis using standardless P/B-ZAF quantification method of film from experiment 1 / Analiza de energie dispersă de raze X (EDX), utilizând metoda de evaluare nestandardizată P/B-ZAF pentru filmul din experimentul 1.

Element	Na	Si	Ca	B	K	S	Cd	O
Norm.C (wt. %)	2.43	28.32	11.33	0.00	10.80	0.14	0.95	46.04
Error	0.2	1.4	0.4	0.00	0.8	0.00	0.3	6.4

wavelength laser is situated in the optical absorption range of CdS-doped glass target. In the case of the film from experiment 2, it is noticed a material composed of structural units having very different shapes and sizes, resulting in a high roughness, possibly due to the low laser energy (1064 nm laser wavelength), placed outside the optical absorption domain of the doped glass.

SEM images show that the morphology of the deposited films is specific to PLD technique, presenting structural units with sizes influenced by the laser energy.

### 3.6. EDX analysis

The EDX analysis shows in evidence the expected dopant constituents, Cd and S besides Ca, K, O, Na, and B, due to the contribution of the vitreous matrix. The presence of a high amount of Si is mainly due to the glass matrix as well as the silicon substrate.

In the Table 3, EDX spectrum of the film from experiment 1 shows the elemental composition after the PLD deposition process and the film from experiments 2 presents the same elemental composition, not reported in this work.

### 3.7. AFM analysis

The surface morphology of the deposited films was investigated by AFM analysis. Figure 6 shows 3D AFM images of CdS-doped films deposited in the experiments 1 and 2. It is to be noticed that the surface morphology of the CdS thin films is strongly dependent on the laser wavelength in the ablation process. In the case of the film from experiment 1, it is observed a rough surface with micron spherulitic units. In the case of the film from experiment 2, the most obvious feature is the occurrence of small size units together with larger size particles, due to 1064 nm wavelength.

The roughness of the film from experiment 1 was estimated at 500 nm and around 220 nm for the film from experiment 2 as it can be observed in the AFM images.

## 4. Conclusions

CdS-doped films have been deposited by PLD method starting from a CdS-doped glass target and changing the pulse number and laser wavelength.

The shift of the optical absorption of the CdS-doped films deposited on quartz substrate toward higher wavelength by comparison with the undoped glass is due to the CdS semiconductor dopant particles having about 4 nm size.

The PL spectra of the glass target and the film from the experiment 2, taken by 450 nm excitation, showed a band in the orange range, specific to CdS defects consisting of cadmium vacancies, sulphur vacancies, interstitial cadmium and sulphur atoms adsorbed on the surface.

Raman spectra revealed that the specific vibration modes of the structural units from the glass target were successfully reproduced in the deposited films.

SEM and AFM images show that the morphology of the deposited films is specific to PLD technique, revealing spherulitic structural units for the films deposited at 248 nm laser wavelength and significant changes appear in the case of the film deposited at 1064 nm. EDX spectra of the films deposited by PLD technique show a well preserved elemental composition by comparison with the glass target.

### Acknowledgments

The authors are grateful to Executive Unity for Financing of Higher Education, Research and Innovation, Romania, for the financial support in the frame of 51/2011 contract from Ideas Program and to Romanian National Authority for Scientific Research by Nucleu Project. No. PN 45N.

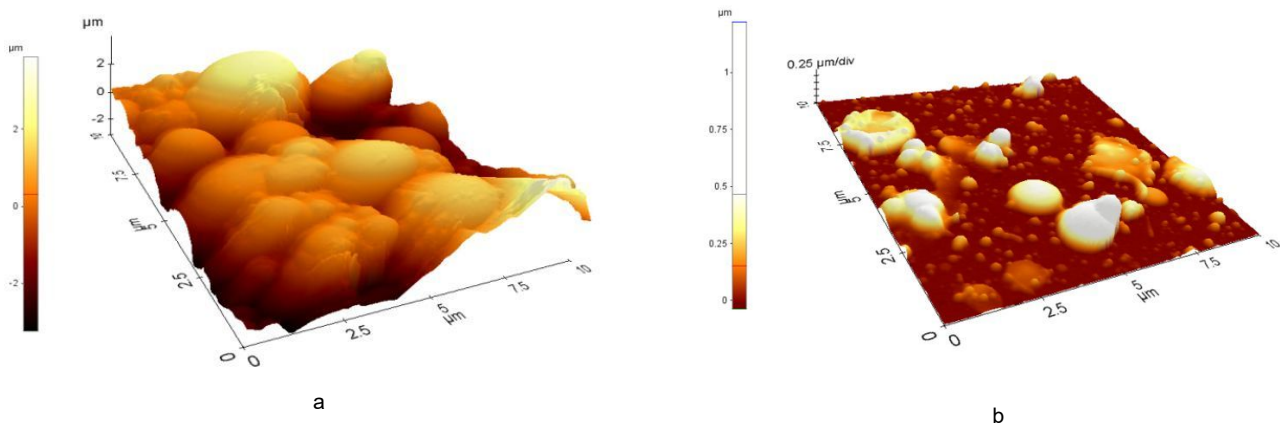


Fig. 6 - 3D AFM images for CdS-doped films deposited on silicon substrate: a) experiment 1; b) experiment 2.

*Imaginile de Microscopie Atomică de Forță (AFM)-3D ale filmelor dopate cu CdS, depuse pe substrat de siliciu: a) experimentul 1; b) experimentul 2.*

## REFERENCES

1. K. Senthil, D. Mangalaraj, S. K. Narayndass, Structural and optical properties of CdS thin films, *Applied Surface Science*, 2010, **169/170**, 476.
2. Q. Wang, G. Xu, G. Han, Solvothermal synthesis and characterization of uniform CdS nanowires in high yield, *Journal of Solid State Chemistry*, 2008, **178**, 2680.
3. Q. Nie, Q. Yuan, W. Chen, Effects of coordination agents on the morphology of CdS nanocrystallites synthesized by the hydrothermal method, *Journal of Crystal Growth*, 2004, **265**, 420.
4. X. Ma, F. Xu, Z. Zhang, Double - dentate solvent – directed growth of multi - armed CdS nanorod - based semiconductors, *Materials Research Bulletin*, 2005, **40**, 2180.
5. Y. Wang, C.Y. To, D.H.L. Ng, Controlled synthesis of CdS nanobelts and the study of their cathodoluminescence, *Materials Letters*, 2006, **60**, 1151.
6. R. Romano, O. L. Alves, Semiconductor / porous glass nanocomposites via the single - source precursor approach, *Materials Research Bulletin*, 2006, **41**, 376.
7. Y. Yang, H. Chen, X. Bao, Synthesis and optical properties of CdS semiconductor nanocrystallites encapsulated in a poly (ethylene oxide) material, *Journal of Crystal Growth*, 2003, **252**, 251.
8. A. Morales-Acevedo, Can we improve the record efficiency of CdS / CdTe solar cells?, *Solar Energy Materials and Solar Cells*, 2006, **90**, 2213.
9. Z. Cheng, F. Su, L. Pan, M. Cao, Z. Sun, CdS quantum dot-embedded silica film as luminescent down-shifting layer for crystalline Si solar cells, *Journal of Alloys and Compounds*, 2010, **494**, L7.
10. I. Feraru, R. Iordănescu, M. Elișa, C. Vasiliu, A. Volceanov, S. Stoleriu, A. Peretz, M. Filipescu, CdSe-doped phosphate glassy films obtained by PLD on silicon substrate, *Chalcogenide Letters*, 2013, **10**, 509.
11. M. Elișa, I. C. Vasiliu, I. D. Feraru, R. Iordănescu, M. I. Rusu, R. D. Trusca, E. Vasile, S. Peretz, CdSe/ZnS-doped silicophosphate films prepared by sol-gel method, *Journal of Sol-Gel Science and Technology*, 2015, **73**, 660.
12. S. Peretz, B. Sava, M. Elișa, G. Stanciu, Cadmium sulphide nanoparticles embedded in polymeric matrices, *Journal of Optical and Advanced Materials*, 2009, **11**(12), 2098.
13. G. Perna, V. Capozzi, S. Pagliara, M. Ambrico, Absorption and photoluminescence analysis of CdS ablated films grown on quartz substrate, *Applied Surface Science*, 2000, **154-155**, 238.
14. M. C. Rao, Growth of metal oxide thin films by Pulsed laser deposition-Perspectives of Pulsed laser ablation mechanism, *Journal of Chemical, Biological and Physical Sciences, Section C*, 2013, **3** (2), 1412.
15. P. Kumar, N. Saxena, R. Chandra, V. Gupta, A. Agarwal, D. Kanjilal, Nanotwinning and structural phase transition in CdS quantum dots, *Nanoscale Research Letters*, 2012, **7**, 584.
16. P. Kumar, N. Saxena, F. Singh, A. Agarwal, Nanotwinning in CdS quantum dots, *Physica B*, 2012, **407**, 3347.
17. H. Wang, Y. Zhu, P. P. Ong, Effect of substrate temperature on the formation of CdO composite in CdS-doped SiO<sub>2</sub> films as deposited by PLD, *Journal of Crystal Growth*, 2002, **241**, 183.
18. H. L. Pushpalatha, S. Bellappa, R. Ganesha, Structural and optical properties of CdS thin film obtained by chemical bath deposition and effect of annealing, *Indian Journal of Pure Applied Physics*, 2015, **52**, 545.
19. M. Thambidurai, N. Murugan, N. Muthukumarasamy, S. Vasantha, R. Balasundaraprabhu, S. Agilan, Preparation and characterization of nanocrystalline CdS thin films, *Chalcogenide Letters*, 2009, **6** (4), 171.
20. D. Pugh-Thomas, B. M. Walsh, M. C. Gupta, CdSe(ZnS) nanocomposite luminescent high temperature sensor, *Nanotechnology*, 2011, **22**, 185503.
21. A. Schuler, M. Python, M. Valle del Olmo, E. de Chambrier, Quantum Dot Containing Nanocomposite Thin Films for Photoluminescent Solar Concentrators, *Solar Energy*, 2007, **81**, 1159.
22. X. S. Zhao, J. Schroeder, P. D. Persans, T. G. Bilodeau, Resonant-Raman-scattering and photoluminescence studies in glass-composite and colloidal CdS, *Physical Review B*, 1991, **43**, 12580.
23. M. Frumar, B. Frumarova, P. Nemeč, T. Wagner, J. Jedelsky, M. Hrdlicka, Thin chalcogenide films prepared by pulsed laser deposition – new amorphous materials applicable in optoelectronics and chemical sensors, *Journal of Non-Crystalline Solids*, 2006, **352**, 544.
24. B. Ullrich, R. Schroeder, Green single- and two-photon gap emission of thin-film CdS formed by infrared pulsed-laser deposition on glass, *IEEE Journal of Quantum Electronics*, 2001, **37**, 1363.
25. X. L. Tong, D.S. Jiang, Y. Li, Z.M. Liu, M.Z. Luo, The influence of the silicon substrate temperature on structural and optical properties of thin-film cadmium sulfide formed with femtosecond laser deposition, *Physica B*, 2006, **382**, 105.
26. H. Aguiar, J. Serra, P. González, B. Leon, Structural study of sol-gel silicate glasses by IR and Raman spectroscopies, *Journal of Non-Crystalline Solids*, 2009, **355**, 475.
27. P. Gonzalez, J. Serra, S. Liste, S. Chiussi, B. Leon, M. Perez-Amor, Raman spectroscopy study of bioactive silica based glasses, *J. Non-Cryst. Solids*, 2003, **320**, 92.
28. P. Nandakumar, C. Vijayan, M. Rajalakshmi, A. K. Arora, Y.V.G.S. Murti, Raman spectra of CdS nanocrystals in Nafion: longitudinal optical and confined acoustic phonon modes, *Physica E*, 2001, **11**, 377.
29. M. Khorasaninejad, J. Walia, S. S. Saini, Enhanced first-order Raman scattering from arrays of vertical silicon nanowires, *Nanotechnology*, 2012, **23**, 275706.
30. P. G. Spizzirri, Probe enhanced, nano-Raman spectroscopy (PERS): A sensitive technique for vibrational surface spectroscopy, *Microscopy: Science, Technology, Applications and Education*, edited by A. Méndez-Vilas and J. Díaz, FORMATEX, 2010, 1393

\*\*\*\*\*